Article

Mechanistic Evaluation of Bioorthogonal Decaging with trans-Cyclooctene: The Effect of Fluorine Substituents on Aryl Azide Reactivity and Decaging from the 1,2,3-Triazoline

Siddharth Sai Matikonda, Jessica M Fairhall, Franziska Fiedler, Suchaya Sanhajariya, Robert A. J. Tucker, Sarah Hook, Anna L. Garden, and Allan B. Gamble

Bioconjugate Chem., **Just Accepted Manuscript** • DOI: 10.1021/acs.bioconjchem.7b00665 • Publication Date (Web): 12 Jan 2018

Mechanistic Evaluation of Bioorthogonal Decaging with *trans*-Cyclooctene: The Effect of Fluorine Substituents on Aryl Azide Reactivity and Decaging from the 1,2,3-Triazoline

Siddharth S. Matikonda,[†] Jessica M. Fairhall,[†] Franziska Fiedler,[†] Suchaya Sanhajariya,[†] Robert A. J. Tucker,[‡] Sarah Hook,[†] Anna L. Garden,[‡] Allan B. Gamble*[,†]

[†]School of Pharmacy, University of Otago, Dunedin, 9054, New Zealand

[‡]Department of Chemistry, University of Otago, Dunedin, 9054, New Zealand

ABSTRACT: Bioorthogonal prodrug activation/decaging strategies need to be selective, rapid and release the drug from the masking group upon activation. The rates of the 1,3-dipolar cycloaddition between a *trans*-cyclooctene (TCO) and a series of fluorine-substituted azido-PABC self-immolative spacers caging two model drugs, and subsequent release from the 1,2,3-triazoline are reported. As the number of fluorine substituents on the PABC linker increases from one to four, the rate of cycloaddition increases by almost one-order of magnitude. Using a combination of fluorescence, $^{1}H/^{19}F$ NMR, and computational experiments we have been able to determine how substituents on the PABC ring can influence the degradation rates and also the product distribution of the 1,2,3-triazoline. We have also been able to determine how these substituents influence the rate of imine hydrolysis and 1,6-self-immolation decaging rates of the generated anilines. The NMR and computational studies demonstrate that fluorine substituents on the aromatic ring lower the transition state energy required for converting the triazoline to the imine or aziridine intermediates via extrusion of diatomic nitrogen, and that in the case of a tetrafluoro substituted aromatic ring, it is the imine hydrolysis and 1,6-self-immolation that is rate-limiting. This knowledge further enhances the understanding of factors which influence the stability of triazolines, and enables potential applications of fluorinated aromatics, in particular perfluorinated aromatics, in synthetic chemistry and sustained-release drug delivery systems.

■ INTRODUCTION

The last fifteen years has seen the rapidly emerging field of bioorthogonal ligations, a class of chemical reactions that can proceed unhindered in the physiological environment, take a prominent role in chemical biology.[1-6] Key to the success of these strategies is a rapid reaction between the bioorthogonal reagents. However, there must be a balance between reactivity and biological stability (bioorthogonality) so that the ligation can be selective and occur before the reaction components are cleared from the biological system.[7] While most research in the field has focused on chemical biology applications; i.e. tracking biomolecules and cells in living systems, more recently, these bioorthogonal chemical reactions have been reported to click-and-release drugs and probes; i.e. to selectively target and activate prodrugs and pro-probes.[8-16] In this emerging sub-field, one of the challenges for *in vivo* applications is the need for sufficiently deactivated prodrugs and pro-probes that are rapidly ligated to the target and subsequently release the active drug/probe on a biologically relevant timescale.[17]

We recently reported a bioorthogonal reaction to decage chemically-masked drugs *via* a strain-promoted 1,3-dipolar cycloaddition between *p*-azidobenzyloxycarbonyl (PABC)-functionalized prodrug/probe and *trans*-cyclooctenol (TCO).[8] The click reaction resulted in second-order rates of 0.017 $M^{-1}s^{-1}$ and 0.027 $M^{-1}s^{-1}$ for the equatorial and axial isomers of TCO, respectively, being at least one-order of magnitude faster than the Staudinger reaction and early examples of strain-promoted azide-alkyne cycloadditions (SPAAC).[18] However, these rates are not sufficiently rapid to accomplish prodrug activation at the low μM concentration of TCO and prodrug that is expected at the tumor site during *in vivo* experiments. To achieve better prodrug and pro-probe activation we require rates to be at least one-to-two orders of magnitude faster than our current system.[19] The rate determining step for our strategy is the 1,3-dipolar cycloaddition, so in designing faster reaction kinetics there is scope to modify the TCO or the azido-PABC-caging linker. Addition of fluorine substituents to the PABC linker, for example as perfluoroaryl azides[20] and tetrafluoroaryl azides[21] results in faster click reactions. Therefore, we chose to investigate the effect of fluorine substituents on our azido-PABC caging linker (Figure 1). As proof-of-concept, 7-hydroxycoumarin **1** and doxorubicin **2** were selected as the model probe and drug for our pro-probe **1a**-**1f** and prodrug **2a**, **2b**, **2d**, and **2e** series, enabling us to examine the rates for the 1,3-dipolar cycloaddition and subsequent decaging from the generated triazoline (five total steps); all of which contribute to prodrug activation and decaging (Scheme 1).[8]

Further mechanistic insight for drug release from the triazoline, determined experimentally and supported by DFT calculations, are reported and build on previous mechanistic studies of 1,3-dipolar cycloadditions between perfluorinated arylazides and enamines or strained dipolarophiles.[20]

Scheme 1. Proposed mechanistic pathway for bioorthogonal activation and degradation/decaging of the PABC linker. Rates 1-5 contribute to the overall decaging process, and the potential rate-determining steps of 1-4 are investigated in this study.

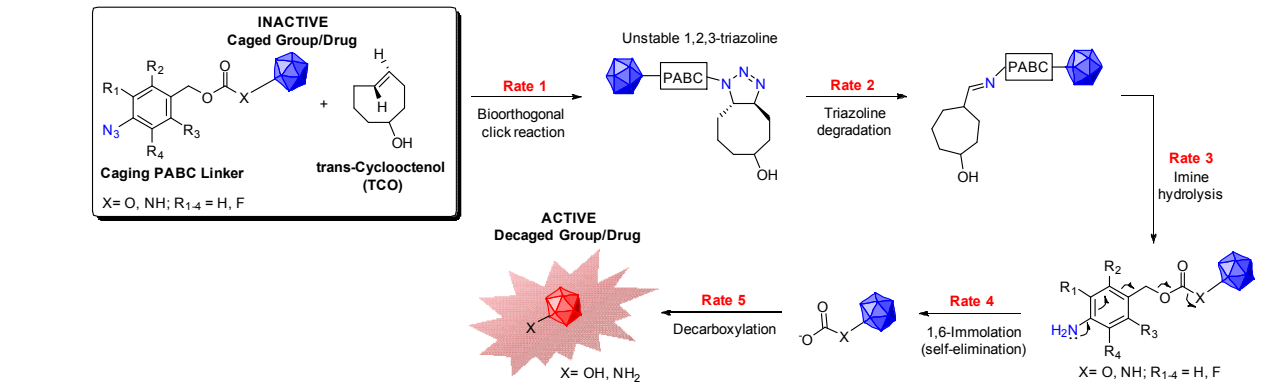

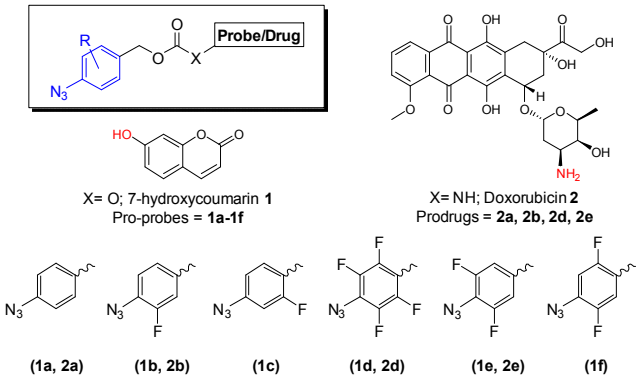

Figure 1. Suite of the fluorinated PABC caging linkers.

According to Sustmann theory,[22, 23] our ambiphilic arylazide is a type II 1,3-dipole, therefore the presence of electron-withdrawing substituents on the 1,3-dipole can reduce the energy gap between the LUMO of the dipole and HOMO of the dipolarophile resulting in a faster click reaction.[21, 23, 24] The negative inductive (-I) effect of fluoro-substitution on the azido-PABC aromatic ring is hypothesized to increase the rate of the 1,3-dipolar cycloaddition. We also envisaged that the electron-withdrawing substituents on the aromatic ring would reduce the nucleophilicity of the nitrogen atom, funnelling the intermediate product towards the imine rather than the aziridine which requires nucleophilic attack of the nitrogen atom at the carbon that extrudes diatomic nitrogen.[25, 26] In addition, the use of fluorine in medicinal chemistry has added benefits[27, 28] of imparting lipophilicity and increasing the binding to serum proteins,[29] and decreasing metabolism of the aromatic ring, both of which aid in improving *in vivo* stability and increasing half-life.[30]

■ RESULTS AND DISCUSSION

Synthesis. Pro-probe analogues of 7-hydroxycoumarin **1a-1f** and doxorubicin prodrugs **2a, 2b, 2d,** and **2e** were synthesized from their corresponding 4-aminobenzyl alcohol **3a-3f** (Scheme 2, Scheme S1). The synthesis of **1a**/**2a** was achieved following the protocols previously reported.[8] 4-Aminobenzyl alcohol **3a** was commercially available, while the other benzyl alcohols **3b-3f** were synthesised from various commercially available starting materials (Scheme 3, Scheme S1). 4-Amino-3,5-difluorobenzyl alcohol **3e** and 4-amino-2,5-difluorobenzyl alcohol **3f** were synthesized from their respective benzyl bromides **6e** and **6f** *via* palladium-catalysed cyanation[31] to afford aryl cyanides **7e** and **7f**, which were further subjected to hydrolysis under alkaline conditions to provide benzoic acids **8e** and **8f**. Benzoic acid **8e** could be directly reduced with $LiAlH_4$ to the benzyl alcohol **3e**, while better overall yields of **3f** were obtained when **8f** was first converted to the corresponding methyl ester **9f** and reduced. 4-amino-3-fluorobenzyl alcohol **3b** and 4-amino-2,3,5,6-tetrafluorobenzyl alcohol **3d** were synthsised by $LiAlH_4$ reduction of the benzoic acids **8b** and **8d**, while 4-amino-2-fluorobenzyl alcohol **3c** was synthesized *via* reduction of the corresponding methyl ester **9c** (Scheme 3, Scheme S1).

Scheme 2. Synthesis of pro-probes 1a-1f and prodrugs 2a, 2b, 2d, and 2e from the corresponding 4-aminobenzyl alcohols 3a-3f.

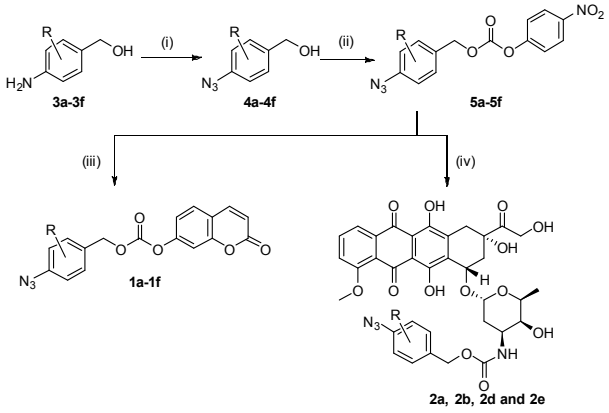

Reagents and conditions: i) $NaNO_2$, 5M HCl and NaN_3, 0°C, 18-98%; ii) *p*-nitrophenyl chloroformate, pyridine, DCM, 25°C, 18-93%; iii) 7-hydroxycoumarin **1**, Et_3N, DMF, 25°C, 63-82%; (iv) Doxorubicin.HCl **2**, Et_3N, 4Å M.S., DMF, 25°C, 49-66%.

Aziridation of **3a-3f** was performed using one of three alternate aziridation conditions (Scheme 2; see Section S2 for alternate procedures). The activated carbonate esters **5a-5f** were synthesized by reacting 4-nitrophenyl chloroformate with the corresponding 4-azidobenzyl alcohols **4a-4f**. Finally, the acyl substitution of **5a-5f** with 7-hydroxycoumarin **1** or the HCl salt of doxorubicin **2** afforded the prodrug analogues **1a-1f** and **2a, 2b, 2d,** and **2e**, respectively.

Scheme 3. Synthesis of benzylalcohols 3b-3f.

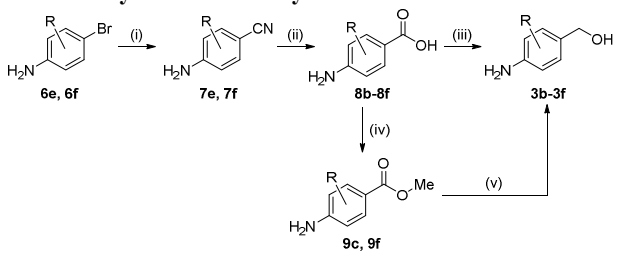

Reagents and conditions: i) $Pd_2(dba)_3$, XPhos, $K_4[Fe(CN)_6]$, NaOAc, dioxane:H_2O (1:1), 25°C, 31 and 95%; ii) KOH, H_2O, 100 °C, 80 and 92%; (iii) $LiAlH_4$, THF, 0-25 °C, 35-55%; (iv) MeOH, H_2SO_4, 65 °C, 54 and 78%; (v) $LiAlH_4$, THF, 0-25 °C, 82 and 84%.

The azido-benzyl ether linked pro-probes **11a** and **11d** were accessed *via* the mesylate of the benzyl alcohol (**10a**, **10d**) and subsequent nucleophilic substitution by 7-hydroxycoumarin **1** (Scheme 4). A modified procedure was used for the synthesis of *trans*-cyclooctenol (TCO) **12**,[32, 33] which resulted in yields higher than that reported in our previous work.

Scheme 4. Synthesis of benzyl ether analogues 11a and 11d

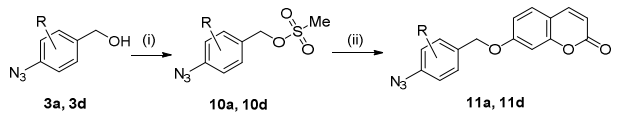

Reagents and conditions: (i) MesCl, Et_3N, DCM (ii) 7-hydroxycoumarin **1**, K_2CO_3, MeCN, 41% (**11a**) and 72% (**11d**).

Release kinetics of prodrug 1a-1f activation. Initial experiments examined the release of 7-hydroxycoumarin **1** from **1a-1f** under the 1:1 mixture of PBS:MeCN conditions we previously reported.[8] The fluorescence of 7-hydroxycoumarin **1** that had been released upon addition of TCO **12** was measured (Figure S1a). Six hours after addition of TCO, 66-100% of **1** was found to be released from **1a-1f** (Figure S1a). In the absence of the trigger (TCO **12**), only a low level of hydrolysis to the carbonate group in **1b-1f** was observed (9-16% at 24 h, Figure S1b). The tetrafluorinated analogue **1d**, that was expected to react fastest in the 1,3-dipolar cycloaddition (Step 1 in Scheme 1), released the lowest amount of **1** at 2 h (20%), indicating that the effect of tetrafluorination may hinder/slow one or all of the subsequent steps in which the linker is still attached to the model drug (Rates 2-4). Also, rates 2-4 could be dependant on solvent, and it may be that a 1:1 mixture of organic and aqueous solvent is not polar enough to promote sufficient triazoline, imine and aniline degradation. Therefore, we investigated the mechanisms along this degradation pathway in greater detail (*vide infra*).

Following the preliminary release experiments, studies on each of the individual steps involved in the activation/decaging process were investigated. The *pseudo* first-order rates (**Rate 1** in Scheme 1) for the 1,3-dipolar cycloaddition between the modified azido-PABC pro-probes **1a-1f** and TCO **12** were determined (Table 1, left column; Figure S2a to Figure S2e). The experiments were conducted in PBS:MeCN (1:1, 37 °C) and the disappearance of the pro-probe **1a-1f** at 254 nm was analysed on RP-HPLC. As hypothesized, the presence of fluoro-groups on the aryl ring resulted in an approximate 2-fold, 4-fold, and 6.5-fold acceleration of the 1,3-dipolar cycloaddition (relative to **1a**) for the mono- (**1b**, **1c**), di- (**1e**, **1f**), and tetrafluoro-substituted analogues (**1d**), respectively. The location of the fluoro-substituents (*ortho*- or *meta*- to the azide) did not greatly affect the rate of 1,3-dipolar cycloaddition.

Next, the effect of the fluoro-substituent pattern on the rate of drug release (**Rates 2-5**, Scheme 1) was examined (Table 1, right column, Figure S4 and S5). We opted for a similar approach to our previous work[8] in which the cycloaddition step was stopped at the triazoline intermediate (in MeCN-d_3) before release of 7-amino-4-methylcoumarin was initiated through a 1000-fold dilution into PBS buffer (measured by spectrofluorometry). However, a slight modification to the experiments was made, in that we examined the release of 7-hydroxycoumarin **1** from the carbonate analogues **1a-1f**, and opted for 100% MeCN-d_3 as solvent in the initial cycloaddition step (*c.f.* 15% DMSO-d_6:MeCN-d_3). The absence of DMSO ensured that anhydrous conditions could be maintained in the initial NMR experiment, while the use of a phenolic leaving group simplified the release kinetics measured in the subsequent dilution experiment. The coumarin phenol **1** is expected to undergo a spontaneous decarboxylation (Rate 5 = secs in Scheme 1), unlike 7-amino-4-methylcoumarin which was recently reported to have a relatively slow decarboxylation (~5 min due to low pKa of protonated aniline).[34]

Table 1. Kinetics of the pro-probes 1a-1f

Entry	[a]Rate of 1,3-dipolar cycloaddition (Rate 1)	[b]Time (min) for 50% release of 1 (Rates 2-5)
1a	0.017 $M^{-1}s^{-1}$ ± 0.003[c]	1.2 ± 0.8
1b	0.035 $M^{-1}s^{-1}$ ± 0.004	4.0 ± 2.2
1c	0.036 $M^{-1}s^{-1}$ ± 0.006	2.4 ± 1.5
1d	0.110 $M^{-1}s^{-1}$ ± 0.036	7.1 ± 1.8
1e	0.067 $M^{-1}s^{-1}$ ± 0.001	5.9 ± 0.4
1f	0.055 $M^{-1}s^{-1}$ ± 0.002	6.9 ± 1.3

[a]Calculated from *pseudo*-first order rate of 1,3-dipolar cycloaddition reaction between **1a-1f** and TCO **12**. [b]The cumulative rate of 1,2,3-triazoline degradation, imine hydrolysis, 1,6-immolation, and decarboxylation shown as steps 2-5 in Scheme 1. [c]Data taken from our previous work.[8] Error represented as ± SD (n = 3).

Briefly, the ^{1}H NMR spectra of the reaction between pro-probes **1a-1f** and TCO **12** were obtained in MeCN-d_3 (Figure 2; Figure S3a to S3f). Following a 20 h reaction, the complete disappearance of the pro-probes **1a-1f** was confirmed and the intermediate triazoline or imine could be observed. Complete conversion to the triazoline was confirmed in all cases (fused ring protons at δ 4.3-4.5 and 3.6-3.9 ppm) except the tetrafluoro-substituted analogue **1d** (Figure 2; Figure S3d) for which transient triazoline peaks (δ 3.5-4.5 ppm) and strong exocyclic imine proton peaks (two isomers) could be observed (δ 8.0 ppm). Table 1 (right column) shows the time required to release 50% of **1** from the triazoline and imine (Scheme 1) when an aliquot from the NMR mixture in MeCN-d_3 was diluted into PBS (1000-fold dilution). *Pseudo* first-order kinetics could be observed over the initial time points measured (Figure S4 and S5), but the complexity of having multiple degra-

dation steps led to a deviation from first-order kinetics, and was particularly evident for analogues **1a-1c**. While the first order rate could not be calculated and directly compared across the series, the maximum observed release, indicated by the plateau of 7-hydroxycoumarin **1** release, occurred within approx. 1 h of dilution (Figure S4 and S5). Interestingly, we observed that sequential addition of fluorine groups on the aryl ring, resulted in a decreased rate of coumarin **1** release as evidenced by the right shift in the release profile for **1b-1f** *c.f.* **1a** (Figure S4). In particular, there was a marked difference observed for the tetrafluoro analogue **1d**, taking approx. 1 h for the release of **1** to reach its plateau; i.e. **1d** with four fluorine groups was the slowest across steps 2-5.

Mechanistic investigation of fluorine substituent effect on triazoline and imine degradation. The results from Table 1 suggest that while fluorine accelerates the 1,3-dipolar cycloaddition, it slows the decaging process. For prodrug activation, the 6.5-fold faster click reaction of the tetrafluoro-substituted azide bodes well for increased localization of the azide prodrug at the desired biological target. However, since we require a click-and-release event, it is critical to understand the mechanism by which substituents on the PABC linker influence the decaging process (Steps 2-4). Not only is this important for mechanistic understanding, but moving forward to *in vivo* models it could provide us with knowledge on how to gain temporal control over the release process, and maybe even lead to sustained-release drug delivery systems.

Electron deficient 1,2,3-triazolines are known to be thermally unstable.[20, 25, 35] Since the triazolines for our analogues **1b-1f** are also electron-poor we hypothesize that the degradation (Scheme 1, Step 2) will not be rate-limiting. Rather the triazolines are expected to be even less stable as the number of fluorine substituents increases. Therefore, we hypothesize that the imine hydrolysis would be the rate-limiting step (Scheme 1, Step 3), especially as the pKa for the nitrogen atom on an aryl imine is lowered in the presence of electron-withdrawing groups,[36] slowing the acid-catalyzed hydrolysis step. The 1,6-self-immolation step could also contribute to the rate, but our expectation was that the elimination would be fast. However, this did not prove to be the case for the analogue containing the tetrafluorinated linker (*vide infra*). Interestingly, recent reports on the Staudinger reaction between tetrafluoroaryl azide and triphenylphosphine resulted in a stable iminophosphorane, making the reaction unsuitable for click-to-release applications.[21] In comparision, the iminophosphorane formed by the reaction of non-substituted aryl azide results in unstable iminophosphoranes.[9,16] This highlights that the hydrolysis of the imine generated from tetrafluoroaryl analogue **1d** could play a significant role in the rate of release.

To test our hypotheses; i.e. the triazoline is destabilised as fluorine substitution increases, and the imine hydrolysis becomes rate-limiting; ^{1}H NMR was used to examine the product distribution for the reaction between pro-probes **1a-1f** and TCO **12** (Figure 2). Analogues **1a-1c, 1e** and **1f** did not exhibit a peak for the imine proton and only 1,2,3-triazoline was evident, but for the tetrafluoro-substituted PABC analogue **1d**, a strong peak corresponding to an imine proton at δ 8.02 ppm was observed (Figure 2, Figures S3a-S3f).

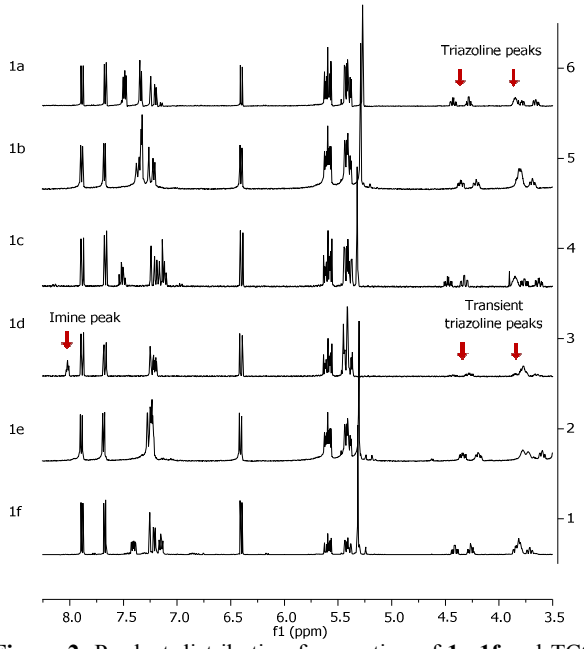

Figure 2. Product distribution for reaction of **1a-1f** and TCO **12** in 100% MeCN-d_3 recorded at 20 h.

The identity of the observed peak at 8.02 was confirmed by ESI+ mass spectral (MS) analysis, with a peak at *m/z* 530.1 assigned as the sodiated molecular ion [M+Na] of the imine ($C_{25}H_{21}F_4NO_6Na$). In the spectrum of **1d**, there was a relatively low abundance of the bridging triazoline proton peaks. From this we can conclude that the presence of four fluorine groups on the PABC ring leads to a relatively unstable 1,2,3-triazoline, even under pure organic solvent conditions (MeCN-d_3), and that the imine hydrolysis could be rate-limiting, especially as fluorine substituents on the ring increase to four.

Further evidence for the proposed stabilization of the imine bond by the four fluorine substituents on the aromatic ring was provided by RP-HPLC analysis. Upon reaction of **1d** with TCO **12,** only a trace amount of released 7-hydroxycoumarin **1** (R_T = 4.9 min) was observed in the HPLC chromatogram (Figure 3). Instead, a major peak at R_T = 7.5 min was visible. In an attempt to confirm the identity of the new peak, the NMR mixture of **1d** containing the imine (from the product distribution experiment in figure 2) was injected onto the HPLC. The NMR mixture showed a retention time matching that of the previously unknown peak at 7.5 min (Figure 3), suggesting the presence of a stable imine. However, when the eluant for the expected imine (R_T = 7.5 min) was collected and re-analysed by MS, the imine molecular ion or its sodiated form was not present, and no conclusive product peak could be identified. Based on all of the experimental evidence (*vide supra*), the presence of a highly stabilized aniline that was present under the HPLC assay conditions and yet to undergo a 1,6-self-elimination, could not be ruled out. The aniline itself could be generated via hydrolysis of the imine upon dilution of the NMR sample in PBS. Of note, release of the coumarin from the imine or the aniline could be influenced by the solvent in a way that an increase in the amount of coumarin released would be expected as the percentage of water/PBS increases. That is, the intermediate imine or aniline is stabilised when there is a relatively high prodrug:proton ratio

(purely organic or organic/aqueous mixture), but destabilized under relatively low prodrug:proton ratio (purely aqueous; expected conditions *in vivo*).

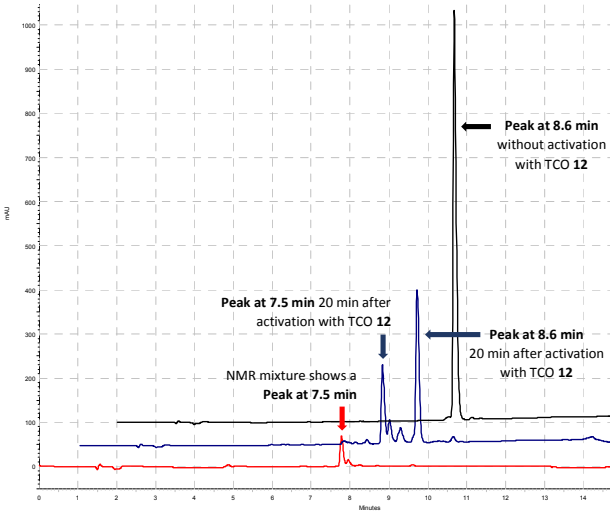

Figure 3. HPLC traces of unidentified peak formed in the reaction of **1d** with **12**. The NMR reaction mixture of **1d** (with confirmed imine), had the same peak at R_T = 7.5 min.

Based on the above NMR and HPLC-UV data, it was evident that the triazoline for the tetrafluorinated analogue **1d** was destabilised by the additional fluorine substituents. However, there was still no direct evidence suggesting which step; imine hydrolysis or 1,6-self-immolation of the aniline, was rate-limiting. To acertain if fluorine substitution could influence the protonation of the imine; i.e. slowing the hydrolysis and release of coumarin, the molecular electrostatic potential (MEP) at the nucleus of the nitrogen atom for the imines of **1a-1f** were computed and correlated to a relative pKa. This quantity has previously been shown to correlate strongly with the experimentally determined pKa such that a more negative MEP corresponds to a larger pKa value.[37] The MEP at the nuclei was calculated *via* the "Prop" keyword in Gaussian09. Table S3 (Section S6) summarises the values of predicted pKa values of the imines corresponding to **1a-1f**. The data demonstrates that the predicted pKa of the imine corresponding to the tetrafluoro-substituted linker **1d** (pKa ~5) is approx. two-orders of magnitude below physiological pH and three-orders of magnitude lower than the imine of the non-substitued analogue **1a** (pKa ~8). The computed data supports the notion that, as the number of fluorine substituents increase the pKa of the imine nitrogen decreases. This means that the tetrafluorinated imine of **1d** is least susceptible to protonation under physiological conditions (pH 7.4), and that acid-catalyzed imine hydrolysis could be, at least in part, responsible for the slow release of coumarin **1** from **1d**.

To further examine the product distribution, imine hydrolysis and 1,6-self-immolation steps experimentally, a series of NMR and fluorescence experiments were conducted using benzyl ether analogues **11a** and **11d** (Figure 4). The benzyl ether linker was selected in order to avoid any background hydrolysis that could occur to the carbonate bond in the corresponding analogues of **1a** and **1d**. In addition, the experiment was designed so that the 1,6-self-immolative step would proceed via a benzyl ether (expected release rate in the order of minutes) instead of the benzyl carbonate (release rate in the order of seconds),[38] enabling a better understanding of the 1,6-self-immolation and its influence on the overall release rate. To quantify the products formed in the reaction of **1d** with **12**, an internal standard (1-Fluoro-2,4-dinitrobenzene) that could be detected by ^{1}H and ^{19}F NMR spectroscopy was added.

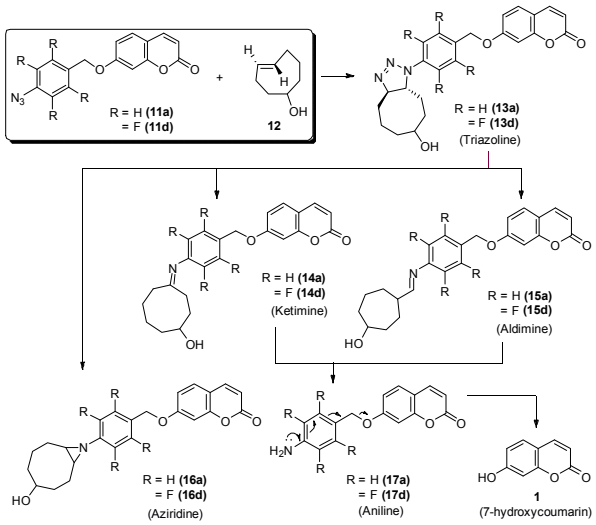

Figure 4. Possible product distribution for benzyl ethers **11a** and **11d** after reaction with TCO **12**. Products of the reaction were monitored by ^{1}H NMR (for **11a** and **11d**) and ^{19}F NMR (for **11d** only).

Initially, the product distribution after addition of TCO **12** to **11a** or **11d** in MeCN-d_3 was monitored by ^{1}H and ^{19}F NMR spectroscopy for 48 h (**11a**) or 72 h (**11d**). It was evident from the ^{1}H and ^{19}F NMR (for **11d** only) spectra, that all of azide **11a** (Figure S9a) and **11d** (Figure 5, 6 and S9b) had been converted to the triazoline **13a** or imine **15d** (confirmed by HRMS analysis with a peak at *m/z* 486.1307; [M+Na]), respectively. While not conclusively identified in the ^{1}H NMR spectrum, aziridine **16d** has the same molecular weight as imine **15d**, thus could also be present in the reaction mixture. In the reaction of **11d** with **12**, the relative integration of imine protons at δ 8.02 ppm did not exhibit the expected 1:1 ratio with the coumarin protons (measured at 72 h; Figure S9b). Instead there was a 1:1.5 relative integration. Closer inspection of the coumarin core proton peaks and the presence of a peak at δ 5.25 ppm, indicated that a structurally related product with similar chemical shifts to the imine was present. The ^{19}F NMR spectrum further supported the presence of other minor products (multiplets at δ -155.8, -154.8, -147.2, -142.6 ppm) in addition to the imine (multiplets at δ -146.1 and -156.8 ppm) and a small amount of remaining triazoline (multiplets at δ -148.8 and -144.6 ppm). We hypothesized that these additional peaks could correspond to the ketimine **14d** or aziridine **16d**. After 72 h (reaction time in NMR tube), a 1000-fold dilution of the reaction mixture containing triazoline **13a** in PBS and monitoring by spectrofluorometry, showed 50% release of **1** in 2.40 ± 0.53 min (Figure S9d), comparable to other 1,6-self-immolative processes for benzyl ethers releasing low pKa phenols.[38, 39] Strikingly, the release from the tetrafluoro-

substituted imine **15d** was ~125× slower, taking ~5 h for 50% of **1** to be released after dilution into PBS (Figure S9d).

To ascertain which step was rate-limiting in the case of **15d** (imine hydrolysis or 1,6-self-immolation) and determine if the additional products were ketimine **14d** or azidirine **16d**, D_2O (10% by volume) was added to the NMR solution (at 72 h). For comparision, D_2O (10% by volume) was also added to the triazoline **13a** (at 72 h). Addition of D_2O to the mixture containing triazoline **13a** resulted in significant release of **1** within 24 h (Figure S9a, 7-hydroxycoumarin peaks illustrated). The aldehyde peak at δ 9.56 ppm indicated that **13a** had, at least in part, released **1** via imine hydrolysis and 1,6-self-immolation via **17a**. Addition of D_2O to the mixture containing **15d** did not result in the release of **1** (Figure 5, S9b), however, an aldehyde peak was present indicating that imine hydrolysis had occurred. Using HRMS analysis, the major product identified in the ^{1}H NMR spectrum was confirmed as aniline **17d** (*m/z* 362.0402; M+Na ion). Closer inspection of the ^{19}F NMR spectrum (Figure 6 and S9c) confirmed one major product with peaks at δ -148.3 and -163.5 ppm (~60% of total ^{19}F integration), which combined with the ^{1}H NMR and HRMS data could be assigned to aniline **17d**. There were some minor products present (~40% of total integration). The second most notable product after D_2O addition, was noted at δ -146.9, -147.2, -158.2, and -158.6. This product starts forming immediately after addition of D_2O, and then slowly decreased over the 96 h period resulting in further formation of aniline **17d**. Therefore, these peaks likely correspond to the enamine tautomer (two possible isomers) of **15d**, which exists in equilibrium with the imine. There was a slight doubling in the peaks of the aromatic region of the ^{1}H NMR spectrum (Figure S9b) at the corresponding time-points, indicating that the enamine has very similar chemical shift values to aniline **17d**. The minor product with peaks centred at δ -147.0 and -155.5 (~15% of total integration) were present in the sample prior to addition of D_2O (note the slight change in chemical shift observed due to change in solvent). Since they were stable under both NMR solvent compositions, the peaks likely correspond to aziridine **16d**, a compound that does not undergo hydrolysis, and not ketimine **14d** or the enamine tautomer of **15d**. Upon addition of D_2O, the multiplets at δ -154.8 and -142.6 ppm disappeared, indicative of ketimine **14d**. The low abundance of these peaks in the original experiment (pre-D_2O) also points towards ketimine **14d**.[25]

Quantification of the products formed from **11d** using the internal standard (1-Fluoro-2,4-dinitrobenzene) was also performed, and supported the initial relative ^{19}F integrations (*vide supra*). Due to chemical shifts of the products/intermediates being very similar in the ^{1}H NMR spectrum, more quantitative information could be gained from the ^{19}F NMR study. After incubating at room temperature for 48 h, the product distribution was; 60% aldimine **15d**, 10% aziridine **16d** (see above for identification), 15% of 1,2,3-triazoline **13d**, and trace amounts **14d**. Prior to addition of D_2O (at 72 h), the product distribution was; 65% aldimine **15d**, 10% aziridine **16d**, 10% of 1,2,3-triazoline **13d**. After D_2O addition (10% by volume) and incubation for 96 h (Figure 6), the product distribution was; 55% aniline **17d**, 10% of aziridine **16d** (unchanged), and 35% of what is suspected to be the enamine tautomer of aldimine **15d**. This result was supported by the ^{1}H NMR spectrum acquired 96 h post D_2O addition (Figure S9b); i.e. 50% of imine hydrolysis evident via presence of aldehyde (δ 9.56 ppm).

The results suggest that the imine hydrolysis does occur quite rapidly under relatively low abundance of water (10% D_2O) for the non-substituted imine (Figure S9a; no imine peak observed and aldehyde peak evident within 5 mins of D_2O addition). As the number of electron-withdrawing fluorine substituents increase, the hydrolysis is slowed (Figure S9b; trace amounts of imine **15d** remain at 24 h post D_2O addition), as predicted by the calculated relative pKa values of the imine nitrogen. The presence of four fluorine atoms on the aryl group would also be expected to increase the electrophilicity of the carbon atom of the imine bond (increasing the hydrolysis rate), but the results suggest that the reduced pKa of the nitrogen dominates (decreasing the hydrolysis rate). However, the overall rate-limiting step in the degradation process of the tetrafluoro-substituted triazoline **13d** and imine **15d**, is likely to be the 1,6-self-immolation of aniline **17d**. One possible explanation for the high stability of **17d** vs the low stability of **17a** could be that shortening of the benzylic carbon-oxygen bond by the electronegative fluorine atoms slows down 1,6-self-immolation, an opposite effect to that reported for addition of electron-donating methoxy aryl ring substituents (bond elongation leading to rapid 1,6-self-immolation).[39]

In summary, the NMR and spectrofluorometry data for **1a-1f**, **11a**, and **11d** suggest that, after the 1,3-dipolar cycloaddition and addition of a protic solvent, the 1,2,3-triazoline **13a/d** is rapidly converted to an aldimine **15a/d** (and enamine), a ketimine **14a/d** and an aziridine **16a/d**. The aldimine/enamine **15a/d** are converted to the aniline **17a/d** via hydrolysis of the aldimine. The rate of imine hydrolysis and the contribution of the 1,6-self-immolation to the overall release rate of coumarin **1** increases as the number of fluorine substituents on the PABC linker increases. For tetrafluoro-substitution (**1d** and **11d**), imine hydrolysis and/or 1,6-self-immolation (especially for benzyl ether **11d**) dominate the observed rate.

Computational analysis of the 1,2,3-triazoline degradation. Triazolines are an important class of compounds used in synthetic chemistry, and there is a significant amount of effort involved in understanding their formation and subsequent degradation mechanisms.[20, 25, 26, 40-47] Therefore, the results obtained in our NMR and HPLC-UV experiments provide an interesting addition to the current mechanistic understanding of triazoline synthesis, stability, and subsequent degradation products. To understand the reason for the instability of the triazoline formed in the case of **1d**/**11d** relative to the triazolines resulting from the cycloaddition of the non-substituted **1a**/**11a** and other fluoro-substituted analogues **1b**, **1c**, **1e**, and **1f**, a mechanistic study was conducted to relate the fluorine substitution to the triazoline degradation and imine hydrolysis. Herein, we discuss the outcome of the computational evaluation and compare this to the experimental observations reported above.

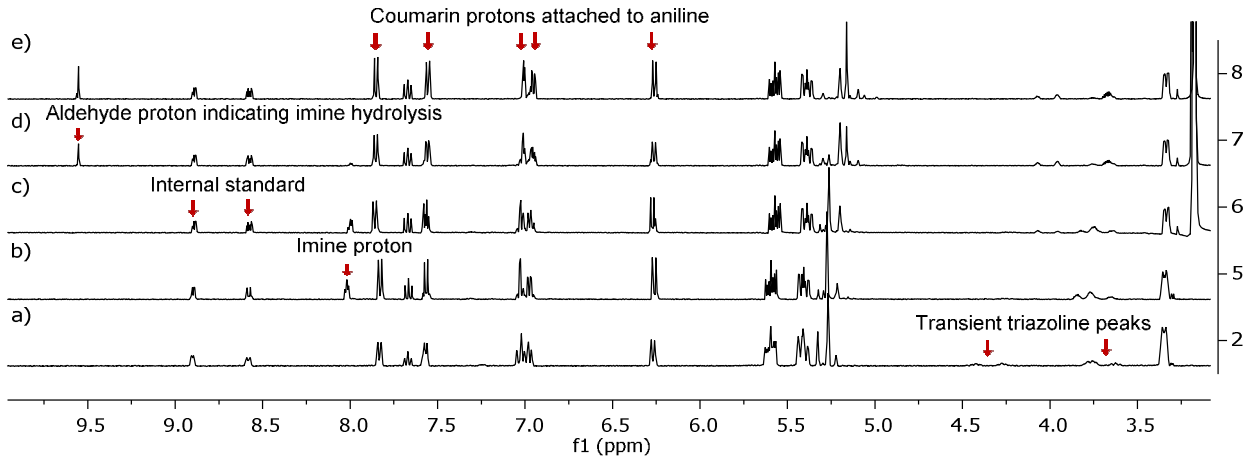

Figure 5. ^{1}H NMR product distribution experiments for reaction of TCO **12** with **11d** a) t = 5 min (MeCN-d_3) b) t = 72 h (MeCN-d_3) c) t = 5 min after adding 10% D_2O d) t = 24 h after adding 10% D_2O e) t = 96 h after adding 10% D_2O.

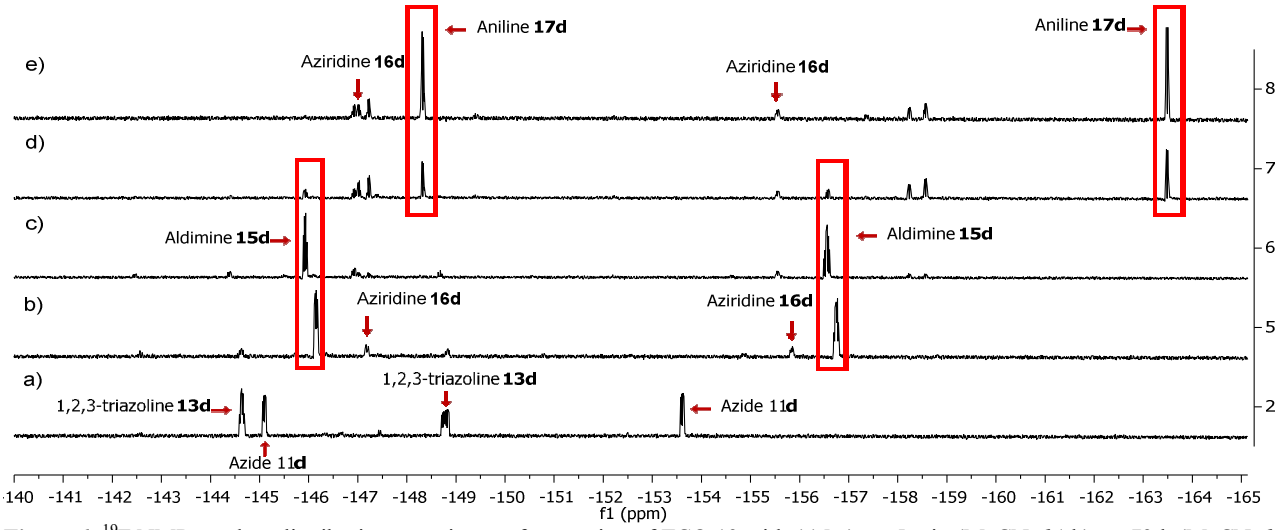

Figure 6. ^{19}F NMR product distribution experiments for reaction of TCO **12** with **11d** a) t = 5 min (MeCN-d_3) b) t = 72 h (MeCN-d_3) c) t = 5 min after adding 10% D_2O d) t = 24 h after adding 10% D_2O e) t = 96 h after adding 10% D_2O.

The relative rates of 1,2,3-triazoline degradation were investigated using *ab initio* techniques (Section S6). Inclusion of implicit solvation was found to have a minimal effect on the thermodynamics of 1,2,3-triazoline (Table S1) therefore simpler, solvent-free methods were used to investigate the kinetics. As the aryl azide is the variable portion of the pro-probes **1a-1f**, a simplified model was used where the 7-hydroxycoumarin and the carbonate group were replaced by a methyl group in the *para*-position with respect to the azide on the linker motif (**18a-18f**; Figure 7). The degradation process was modelled by the elementary reaction step of the ring opening (Figure 7).

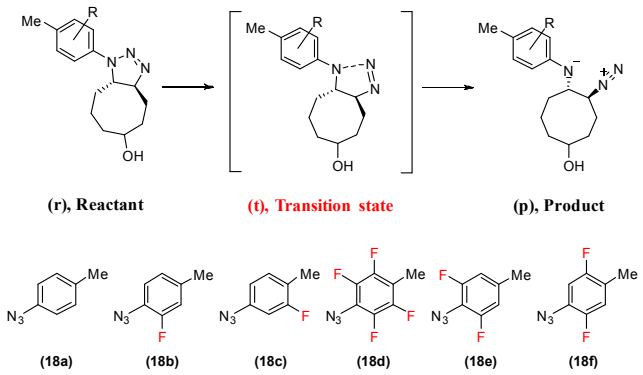

Figure 7. Elementary step chosen to model 1,2,3-triazoline degradation.

Transition states of the triazoline degradation were identified using a relaxed surface scan through the NNN angle, refined using the QST3 method and confirmed using frequency and IRC calculations (Refer to Table S2 for the coordinates and energies of the transition states of 1,2,3-triazoline degra-

dation). Table 2 summarises the energetics and relative rates of the triazoline degradation. Evidently the triazoline corresponding to **18d** is highly unstable with a 27000-fold (four-orders in magnitude) higher k_{rel} than **18a** (Figure S8). Additionally, **18e** and **18f** were computed to have a 60 to 600-fold (approximately one to two-orders in magnitude) higher k_{rel} than **18a**. Hence, it can be concluded that introducing the fluorine group onto the aryl ring of the PABC linker destabilizes the 1,2,3-triazoline and increases the rates of triazoline degradation. This supports the experimental data obtained in the $^{1}H/^{19}F$ NMR and fluorometry studies (*vide supra*).

Table 2. Energetics and computed k_{rel} of 1,2,3-triazoline degradation

Entry	ΔG / kJ mol^{-1}	G_a / kJ mol^{-1}	k_{rel} (298 K)
18a	126	199	1
18b	123	194	9
18c	124	194	9
18d	112	174	27268
18e	119	183	585
18f	120	189	62

$\Delta G = G_{product} - G_{reactant}$, $G_a = G_{transition\ state} - G_{reactant}$

Cytotoxicity of TCO-activated doxorubicin-based prodrugs 2a, 2b, 2d, and **2e**. Based on the kinetics reported in Table 1, the number of fluorine groups on the PABC linker determines the kinetics of drug/probe decaging irrespective of its position on the aromatic ring. Hence, we analysed the doxorubicin prodrugs **2a, 2b, 2d,** and **2e** to examine if activation by 1,3-dipolar cycloaddition restored the cytotoxicity of doxorubicin **2** against a B16-OVA melanoma cell culture (**Table 3)**. After 48 h incubation in the presence of TCO **12** (100 μM), varying degrees of activity were restored, indicating activation of the prodrug and subsequent release of free doxorubicin **2**. In the absence of TCO **12**, prodrugs **2a, 2b, 2d,** and **2e** were 10-to-35-fold less toxic to the melanoma cells, indicating that the azido-PABC linkers deactivate doxorubicin and are relatively stable *in vitro* over 48 h. Notably, the tetrafluoro-substituted prodrug **2d** had the highest IC_{50} (>50 μM) of all prodrugs, but upon activation full activity of doxorubicin **2** was not restored (5.97 μM vs. 0.84 μM). This may be a result of slow aldimine hydrolysis or 1,6-self-immolation of the aniline derivative, as previously demonstrated for coumarin analogues **1d** and **11d**.

Based on our fluorescence experimental results with **1d** and **11d**, the release under a protic solvent should still be relatively rapid (minutes to hours), and the 48 h incubation should have been sufficient time for complete release of doxorubicin **2**. Therefore, the reason for not seeing complete conversion of the prodrug **2d** to doxorubicin **2** may lie in the fact that four fluorine atoms impart a high lipophilicity on the prodrug **2d** and the intermediate aldimine and aniline. In this situation, the imine and aniline may diffuse more readily into the lipid bilayer of the cells (favoured equilibrium) where the proton source is low and hence imine protonation and 1,6-self-immolation is slowed.

Table 3. Cytotoxicity study of TCO **12** activated prodrugs **2a, 2b, 2d,** and **2e** against B16-OVA melanoma cells.

Entry	IC_{50}[a,b,c] (μM)	IC_{50}[a,b,c] (μM) on activation with TCO
Doxorubicin	0.84 (0.79 – 0.89)	-
2a	29.40 (11.64 – 74.28)	1.39 (1.25 – 1.53)
2b	37.00 (19.43 – 70.46)	1.06 (0.95 – 1.17)
2d	>50	5.97 (4.68 – 7.60)
2e	32.95 (19.06 – 56.97)	0.98 (0.88 - 1.09)

[a]IC_{50} values for doxorubicin **2**, prodrugs **(2a, 2b, 2d,** and **2e)** and activation of the prodrugs with TCO **12** (100 μM), incubated for 48 h at 37 °C. [b]IC_{50} = concentration required to kill 50% of cells. [c]95% confidence interval (n ≥ 3) in parenthesis.

■ CONCLUSIONS

The effect of fluorine-substitution on aromatic azides that take part in a potentially bioorthogonal 1,3-dipolar cycloaddition with TCO **12** has been investigated. The role of the fluorine substituents on the kinetics of the reaction and subsequent release/decaging of the PABC linker from a drug or probe have been discussed, and key mechanistic insights have been made. The rate of the cycloaddition increased upon sequential addition of fluoro-substituents, with a maximum rate of 0.110 $M^{-1}s^{-1}$ achieved in the tetrafluoro-substituted analogue **1d**, an approximate order-of-magnitude improvement over the non-substituted linker **1a**. However, the opposite trend was observed for the subsequent release/decaging step; i.e. as fluorine-substitution increased, the rate of release/decaging slowed. Spectrofluorometry, NMR and computational studies demonstrated that the slower release/decaging was a result of the electronegative fluorine atoms, which stabilize the intermediate aldimine, and in the case of the tetrafluorinated aryl azides, the aniline that is primed for 1,6-self-immolation. Doxorubicin prodrugs caged with the fluorinated aryl azides **2a, 2b, 2d,** and **2e** were relatively inactive against a melanoma cell line, and upon reaction with TCO **12** were decaged, and cytotoxicity of the parent doxorubicin was almost entirely restored, except for the tetrafluorinated prodrug **2d**. We are currently investigating the use of these and other caging groups in *in vitro* and *in vivo* pre-targeting strategies (TCO-antibody conjugates). Our lab is also investigating the use of fluorinated PABC caging groups in sustained-release drug delivery. Lastly, as part of our investigation we were able to examine the stability of 1,2,3-triazolines (experimentally and computationally), and the subsequent product distribution following degradation of the ring. This adds mechanistic insight into the degradation process, and complments the work of others in this area.[20, 25, 26, 40-47] Due to the importance of the triazoline in organic chemistry, this provides valuable information for synthetic chemists, enabling them to design triazolines of varying stability.

■ EXPERIMENTAL METHODS

Spectrofluorometry Release Experiments (Section S3). *In a typical experiment:* Stock solutions of coumarin probe **1a-1f** (5 mM, **Stock A**), in MeCN and TCO **12** (50 mM, **Stock B**), in MeCN were prepared. A solution of PBS:MeCN was prepared to a volume of 800 μL (500 μL PBS and 300 μL MeCN), to which, 100 μL of **Stock A** was added (resulting in a volume of 900 μL). In the case of control studies, 100 μL of MeCN was added to the result in a total volume of 1 mL (0.5 mM of the coumarin probe). To begin the release experiments,

100 μL of **stock B** was added for a final volume of 1 mL (1:1 PBS:MeCN), a 0.5 mM solution of coumarin probe and a 5 mM solution of TCO **12**. The solutions (including the control runs) were incubated at 37 °C and at relevant time points, a 50 μL aliquot was taken from the incubated solutions and diluted in PBS (2950 μL, 60× dilution). The PBS solution was vortexed briefly, transferred to a plastic cuvette and the fluorescence measured at 455 nm (Ex 360 nm). The experiment was repeated for a total of three runs (n = 3). The amount of **1** released was calculated from a standard curve.

HPLC Kinetic Experiments - 1,3-Dipolar Cycloaddition (Section S4). A stock of TCO **12** in MeCN was prepared at 100 mM or 200 mM, and a 7-hydroxycoumarin probe **1a-1f** stock was prepared at 5mM in MeCN (**Stock A**). For the control experiment (run in triplicate), 100 μL of coumarin probe **1a-1f** stock (**Stock A**, in MeCN) was added to a solution containing 400 μL MeCN and 500 μL PBS (total volume of 1 mL). From this solution was taken a 50 μL aliquot, which was diluted into a 950 μL solution of PBS:MeCN (1:1) in an HPLC vial. The solution was injected onto the HPLC (inj. vol. 50 μL) at t = 0 min. The control was then incubated at 37 ^{o}C for 240 mins before a further aliquot was taken and measured by HPLC-UV at 254 nm (this was run in triplicate).

To begin the 1,3-dipolar cycloaddition reaction, 100 μL of the TCO **12** stock was added to a vial containing 100 μL of the coumarin probe stock (**Stock A**), 300 μL MeCN and 500 μL PBS. The reaction was incubated at 37 °C and at the time points indicated, a 50 μL aliquot was taken and diluted in a 950 μL solution of PBS:MeCN (1:1). The solution was injected onto the HPLC (inj. vol. 20 μL or 50 μL), and the disappearance in absorbance for the coumarin probe **1a-1f** was measured at 254 nm (triplicate experiments). From the *pseudo* first-order plots, the second-order rates could be calculated using the concentration of TCO **12** (5 mM, 10 mM or 20 mM).

Spectrofluorometry Kinetic Experiments - Triazoline and Imine Degradation 1a-1f (Section S5). *In a typical experiment:* Stock solutions of coumarin probe **1a-1f** (40 mM, **Stock C**), in MeCN-d_3 and **12** (50 mM, **Stock B**), in MeCN-d_3 were prepared. An aliquot was taken from the **Stock C** (130 μL) and added to an NMR tube containing 195 μL of MeCN-d_3. To start the 1,3-dipolar cycloaddition reaction, 325 μL of **Stock B** was added to the mixture (shaken well for 5 secs), and analysed by NMR spectroscopy. The addition of the stocks resulted in a final concentration of 8 mM for coumarin probe **1a-1f** and 25 mM of **12**. The NMR sample was incubated at 25 °C and the progress was measured at 0 h and 20 h. After 20 h of incubation, the ^{1}H NMR spectra indicated that all of the azide had reacted and that conversion of the coumarin probe to the corresponding triazoline or imine had occured (See Figure S3a – S3f).

An aliquot of the NMR sample containing triazoline (3 μL) was further diluted into PBS (2997 μL, 1000-fold dilution; resulting in 8 μM of the coumarin pro-probe), starting the triazoline/imine degradation. The PBS solution was vortexed briefly, transferred to a plastic cuvette and the fluorescence was scanned over 3600 seconds at 455 nm (ex. 360 nm). The experiment was repeated for a total of three runs (n = 3). From the standard curve of 7-hydroxycoumarin **1** (Figure S6), the maximum amount of **1** release from pro-probes was calculated to be 1146.63 units (8 μM). The plots from the time-scan on spectrometer were plotted and the 50% release was calculated using GraphPad Prism 7 software. (Figure S4)

Computational Studies (More details in Section S6). Initial structures were generated using a Monte Carlo conformer distribution search performed in Spartan '14[48] with a Merck molecular force field (MMFF06).[49] This was performed only for **18e** and other molecules were built from this one. 10,000 conformers were searched and the lowest energy conformer was retained for further calculation. This conformer was found to account for either a very high proportion of the population at 298 K (>96 %) or, in the case of other low-lying conformers, the structures were very similar near the triazoline and varied only further out on the probe. Minima and transition states were optimised using density functional theory (DFT) with the B3LYP functional and the 6-31G+(d) basis set with the Gaussian 09 program suite.[50] Vibrational frequency calculations were performed to confirm either minima (no imaginary frequencies) or transition states (one imaginary frequency) had been found. Intrinsic reaction coordinate (IRC) calculations were performed to ensure the TS connected the relevant minima.

Relative rates of 1,2,3-triazoline degradation were investigated by using a simplified model (Figure 7) where the probe and carbonate group were replaced by a methyl group at the *para*-position on the PABC-linker. The degradation process was modelled by the elementary reaction step of the ring opening, as shown in (Figure 7). The difference between the transition state and reactant energies of this step was taken as the activation energy and a constant prefactor was assumed for all linkers. Transition states were identified using a relaxed surface scan through the NNN angle, refined using the QST3 method and confirmed using frequency and IRC calculations.

To calculate the MEP at the nucleus, the "Prop" keyword is added to the root section of a calculation. This keyword directs Gaussian to compute electrostatic properties. By default, the potential, electric field, and electric field gradient at each nucleus are computed. The density used for the electrostatic analysis is controlled by the "density" keyword. MEP values are converted to pKa values based on an empirical relationship established by Liu and Pedersen[37] based on the measured pKa and computed MEP of 154 amines and anilines (see SI). Note that the relationship only holds for N atoms and different relationships exist for other atom types.

^{1}H NMR studies of bioorthogonal activation of the pro-probes 11a and 11d: A 10 mM stock of the 7-hydroxycoumarin pro-probes **11a** and **11d** in MeCN-d_3, 250 mM solution of the internal standard (1-fluoro-2,4-dinitrobenzene) and a 935 mM stock of TCO **12** in MeCN-d_3 were prepared. 500 μL of coumarin (**11a** and **11d**) stock, 20 μL of the interal standard was further diluted with 210 μL of MeCN-d_3. To begin the 1,3-dipolar cycloaddition, 20 μL of TCO **12** stock was added (resulting in a final concentation of 24.93 mM of **12** and 6.67 mM of the coumarin probe and the internal standard; the mixture was incubated in the dark at room temperature). For 48 h (for **11a**) and 72 h (for **11d**), the reaction progress was analysed *via* ^{1}H NMR spectroscopy at room temperature to ensure conversion to the corresponding triazoline **13a** (from **11a**) or aldimine **15d** (from **11d**). And upon complete conversion, 75 μl of D_2O was added to the sample to initiate triazoline and imine degradation; NMR samples were measured at indicated time points.

Similar to spectrofluorometry kinetic studies, a 3 µL aliquot of the NMR sample (before the addition of D_2O) was diluted into 2997 µL of PBS to initiate triazoline degradation, imine hydrolysis and 1,6-elimination which was measured by spectrofluorometry time-scan over 3600 seconds for **11a** and various time points over 2 days for **11d** at excitation 360 nm and emission 455 nm. The time for 50% release was calculated to be 2.40 ± 0.53 minutes (n=3). The time for 50% release from tetrafluoro-substituted linker was calculated to be ~4.83 hours (n=2).

Cell Culture and Proliferation Assay: The murine B16-OVA melanoma cells were maintained in a humidified CO_2 (5%) incubator (Heraeus) at 37 °C in RPMI-1640 media (Gibco), supplemented with 10% fetal bovine serum (FBS) (Gibco), 1% GlutaMAX (Gibco), 1% Pen Strep (Gibco) and 0.1% 2-Mercaptoethanol (55 mM) (Gibco). Cells were plated out in flat bottom 96-well plates (BD Falcon) at a density of 7500 cells/well and allowed to attach for 24 h. The doxorubicin prodrugs **2a, 2b, 2d,** and **2e** were dissolved in DMSO at 10 mM and subsequently serial-diluted in pre-warmed culture media. TCO **12** was dissolved in DMSO at 100 mM and diluted to 200 µM in pre-warmed culture media. After 24 h cell attachment, cell culture medium was replaced by 50 µL pre-warmed media containing the compounds in different concentrations and 50 µL pre-warmed media containing **12** at 200 µM (final concentration in each well was 100 µM). After 48 h incubation, cell proliferation was assessed by means of a MTT assay.

Thiazolyl Blue Tetrazolium Bromide (MTT) (Sigma Aldrich) was freshly dissolved in PBS at 5 mg/mL, passed through a 0.22 µm filter, and 10 µL were added to each well. After an incubation period of 4 h, the medium was gently removed. The formed formazan crystals were dissolved in 100 µL DMSO (Sigma Aldrich), subsequently the absorbance was measured with a plate reader (PolarStar Omega, BMG Labtech)) at 570 nm. As a reference wavelength (background), 690 nm was chosen and subtracted from the absorbance at 570 nm. The cytotoxicity assay was performed in at least three independent experiments, with duplicate experiments on each plate (i.e. 2 x 3 wells per drug/prodrug concentration in each of the independent experiments for a total of $n \geq 3$. IC_{50} values were calculated using the normalized (variable) dose-response parameters in GraphPad Prism 7 software (Figure S10).

■ ASSOCIATED CONTENT

Supporting Information. Synthetic procedures and characterization of compounds **1b-1f**, **2b**, **2d**, **2e**, **11a**, **11d** and all intermediates, ^1H and ^{13}C NMR spectra of final compounds, supplementary figures and tables, coordinates and energies of transition states. This material is available free of charge *via* the Internet at http://pubs.acs.org.

■ AUTHOR INFORMATION

Corresponding Author
*Email: allan.gamble@otago.ac.nz

Notes
The authors declare no competing financial interest.

Funding Sources
This research was supported by a contract from the Health Research Council of New Zealand (A.B.G).

■ ACKNOWLEDGMENT

The authors would like to thank the NMR and MS facility at Department of Chemistry (Otago) for allowing us to use their facilities, Dr Pummy Kritaphol for technical support with HPLC experiments and the Health Research Council (HRC) for a doctoral scholarship (J.M.F).

■ REFERENCES

(1) Sletten, E. M. and Bertozzi, C. R. (2009) Bioorthogonal chemistry: Fishing for selectivity in a sea of functionality. *Angew. Chem. Int. Ed. 48*, 6974-6998.
(2) Saxon, E. and Bertozzi, C. R. (2000) Cell surface engineering by a modified staudinger reaction. *Science 287*, 2007-2010.
(3) King, M. and Wagner, A. (2014) Developments in the field of bioorthogonal bond forming reactions – Past and present trends. *Bioconjugate Chem. 25*, 825-839.
(4) Prescher, J. A. and Bertozzi, C. R. (2005) Chemistry in living systems. *Nat. Chem. Biol. 1*, 13-21.
(5) Bertozzi, C. R. (2011) A decade of bioorthogonal chemistry. *Acc. Chem. Res. 44*, 651-653.
(6) Ramil, C. P. and Lin, Q. (2013) Bioorthogonal chemistry: strategies and recent developments. *Chem. Commum. 49*, 11007-11022.
(7) Sletten, E. M. and Bertozzi, C. R. (2011) From mechanism to mouse: a tale of two bioorthogonal reactions. *Acc. Chem. Res. 44*, 666-676.
(8) Matikonda, S. S., Orsi, D. L., Staudacher, V., Jenkins, I. A., Fiedler, F., Chen, J., and Gamble, A. B. (2015) Bioorthogonal prodrug activation driven by a strain-promoted 1,3-dipolar cycloaddition. *Chem. Sci. 6*, 1212-1218.
(9) Brakel, R. V., Vulders, R. C. M., Bokdam, R. J., Grüll, H., and Robillard, M. S. (2008) A doxorubicin prodrug activated by the Staudinger reaction. *Bioconjugate Chem. 19*, 714-718.
(10) Xu, M., Tu, J., and Franzini, R. M. (2017) Rapid and efficient tetrazine-induced drug release from highly stable benzonorbornadiene derivatives. *Chem. Commun. 53*, 6271-6274.
(11) Versteegen, R. M., Rossin, R., Ten Hoeve, W., Janssen, H. M., and Robillard, M. S. (2013) Click to release: Instantaneous doxorubicin elimination upon tetrazine ligation. *Angew. Chem. Int. Ed. 52*, 14112-14116.
(12) Weiss, J. T., Dawson, J. C., Fraser, C., Rybski, W., Torres-Sánchez, C., Bradley, M., Patton, E. E., Carragher, N. O., and Unciti-Broceta, A. (2014) Development and bioorthogonal activation of palladium-labile prodrugs of gemcitabine. *J. Med. Chem. 57*, 5395-5404.
(13) Weiss, J. T., Dawson, J. C., Macleod, K. G., Rybski, W., Fraser, C., Torres-Sánchez, C., Patton, E. E., Bradley, M., Carragher, N. O., and Unciti-Broceta, A. (2014) Extracellular palladium-catalysed dealkylation of 5-fluoro-1-propargyl-uracil as a bioorthogonally activated prodrug approach. *Nat. Commun. 5*, 3277.
(14) Ritter, C., Nett, N., Acevedo-Rocha, C. G., Lonsdale, R., Kraling, K., Dempwolff, F., Hoebenreich, S., Graumann, P. L., Reetz, M. T., and Meggers, E. (2015) Bioorthogonal enzymatic activation of caged compounds. *Angew. Chem. Int. Ed. 54*, 13440-13443.
(15) Van de Bittner, G. C., Bertozzi, C. R., and Chang, C. J. (2013) Strategy for dual-analyte luciferin imaging: In vivo bioluminescence detection of hydrogen peroxide and caspase activity in a murine model of acute inflammation. *J. Am. Chem. Soc. 135*, 1783-1795.
(16) Gorska, K., Manicardi, A., Barluenga, S., and Winssinger, N. (2011) DNA-templated release of functional molecules with an azide-reduction-triggered immolative linker. *Chem. Commun. 47*, 4364-4366.

(17) Zawilska, J. B., Wojcieszak, J., and Olejniczak, A. B. (2013) Prodrugs: a challenge for the drug development. *Pharmacol. Rep. 65*, 1-14.
(18) Lang, K. and Chin, J. W. (2014) Bioorthogonal reactions for labeling proteins. *ACS Chem. Biol. 9*, 16-20.
(19) Selvaraj, R. and Fox, J. M. (2013) *trans*-Cyclooctene — a stable, voracious dienophile for bioorthogonal labeling. *Curr. Opin. Chem. Biol. 17*, 753-760.
(20) Xie, S., Lopez, S. A., Ramström, O., Yan, M., and Houk, K. N. (2015) 1,3-Dipolar cycloaddition reactivities of perfluorinated aryl azides with enamines and strained dipolarophiles. *J. Am. Chem. Soc. 137*, 2958-2966.
(21) Sundhoro, M., Jeon, S., Park, J., Ramström, O., and Yan, M. (2017) Perfluoroaryl azide Staudinger reaction: A fast and bioorthogonal reaction. *Angew. Chem. Int. Ed. 56*, 12117-12121.
(22) Sustmann, R. and Trill, H. (1972) Substituent effects in 1,3-dipolar cycloadditions of phenyl azide. *Angew. Chem. Int. Ed. 11*, 838-840.
(23) Sustmann, R. (1971) A simple model for substituent effects in cycloaddition reactions. I. 1,3-dipolar cycloadditions. *Tetrahedron Lett. 12*, 2717-2720.
(24) Jewett, J. C. and Bertozzi, C. R. (2010) Cu-free click cycloaddition reactions in chemical biology. *Chem. Soc. Rev. 39*, 1272-1279.
(25) Shea, K. J. and Kim, J. S. (1992) Influence of strain on chemical reactivity. Relative reactivity of torsionally strained double bonds in 1, 3-dipolar cycloadditions. *J. Am. Chem. Soc. 114*, 4846-4855.
(26) Cases, M., Duran, M., Mestres, J., Martín, N., and Solà, M. (2001) Mechanism of the addition reaction of alkyl azides to [60]fullerene and the subsequent N_2 Extrusion to form monoimino-[60]fullerenes. *J. Org. Chem. 66*, 433-442.
(27) Gillis, E. P., Eastman, K. J., Hill, M. D., Donnelly, D. J., and Meanwell, N. A. (2015) Applications of fluorine in medicinal chemistry. *J. Med. Chem. 58*, 8315-8359.
(28) Zhou, Y., Wang, J., Gu, Z., Wang, S., Zhu, W., Acena, J. L., Soloshonok, V. A., Izawa, K., and Liu, H. (2016) Next generation of fluorine-containing pharmaceuticals, compounds currently in Phase II-III clinical trials of major pharmaceutical companies: New structural trends and therapeutic areas. *Chem. Rev. 116*, 422-518.
(29) Meanwell, N. A. (2011) Synopsis of some recent tactical application of bioisosteres in drug design. *J. Med. Chem. 54*, 2529-2591.
(30) Böhm, H. J., Banner, D., Bendels, S., Kansy, M., Kuhn, B., Müller, K., Obst-Sander, U., and Stahl, M. (2004) Fluorine in medicinal chemistry. *ChemBioChem 5*, 637-643.
(31) Senecal, T. D., Shu, W., and Buchwald, S. L. (2013) A general, practical palladium-catalyzed cyanation of (hetero)aryl chlorides and bromides. *Angew. Chem. Int. Ed. 52*, 10035-10039.
(32) Inoue, T., Matsuyama, K., and Inoue, Y. (1999) Diastereodifferentiating *Z-E* photoisomerization of 3-benzoyloxycyclooctene: Diastereoselectivity switching controlled by substrate concentration through competitive intra- vs intermolecular photosensitization processes. *J. Am. Chem. Soc. 121*, 9877-9878.
(33) Royzen, M., Yap, G. P., and Fox, J. M. (2008) A photochemical synthesis of functionalized *trans*-cyclooctenes driven by metal complexation. *J. Am. Chem. Soc. 130*, 3760-3761.
(34) Alouane, A., Labruère, R., Le Saux, T., Aujard, I., Dubruille, S., Schmidt, F., and Jullien, L. (2013) Light activation for the versatile and accurate kinetic analysis of disassembly of self-immolative spacers. *Chem. Eur. J. 19*, 11717-11724.
(35) Chow, A. H., Chiu, F. C., Damani, L. A., and Kadaba, P. K. (1996) Triazolines. 34. Structure and stability relationships of novel Δ^2-1,2,3-triazoline anticonvulsants. *Pharm. Res. 13*, 179-182.
(36) Morgenthaler, M., Schweizer, E., Hoffmann-Röder, A., Benini, F., Martin, R. E., Jaeschke, G., Wagner, B., Fischer, H., Bendels, S., Zimmerli, D., et al. (2007) Predicting and tuning physicochemical properties in lead optimization: Amine basicities. *ChemMedChem 2*, 1100-1115.
(37) Liu, S., Schauer, C. K., and Pedersen, L. G. (2009) Molecular acidity: A quantitative conceptual density functional theory description. *J. Chem. Phys. 131*, 3648.
(38) Matikonda, S. S., Fairhall, J. M., Tyndall, J. D. A., Hook, S., and Gamble, A. B. (2017) Stability, kinetic, and mechanistic investigation of 1,8-self-immolative cinnamyl ether spacers for controlled release of phenols and generation of resonance and inductively stabilized methides. *Org. Lett. 19*, 528-531.
(39) Schmid, K. M., Jensen, L., and Phillips, S. T. (2012) A self-immolative spacer that enables tunable controlled release of phenols under neutral conditions. *J. Org. Chem. 77*, 4363-4374.
(40) Hamadouche, M., Gaudel-Siri, A., Pons, J. M., and Abed, D. E. (2010) Relative stability of a series of 1,2,3-triazolines. Theoretical study of substituent effects. *J. Mol. Struc.: THEOCHEM 956*, 33-37.
(41) Bodnar, B. S. and Miller, M. J. (2007) Reactions of nitroso hetero-Diels−Alder cycloadducts with azides: Stereoselective formation of triazolines and aziridines. *J. Org. Chem. 72*, 3929-3932.
(42) Contini, A. and Erba, E. (2012) Click-chemistry approach to azacycloalkene monosulfonyl diamines: synthesis and computational analysis of the reaction mechanism. *RSC Adv. 2*, 10652-10660.
(43) Wladkowski, B. D., Smith, R. H., and Michejda, C. J. (1991) Theoretical investigation of the proton-induced decomposition of 4,5-dihydro-1,2,3-triazole to form the aziridinium ion: instability of the (2-aminoethyl)diazonium ion. *J. Am. Chem. Soc. 113*, 7893-7897.
(44) Audran, G., Adiche, C., Brémond, P., El Abed, D., Hamadouche, M., Siri, D., and Santelli, M. (2017) Cycloaddition of sulfonyl azides and cyanogen azide to enamines. Quantum-chemical calculations concerning the spontaneous rearrangement of the adduct into ring-contracted amidines. *Tetrahedron Lett. 58*, 945-948.
(45) Chung, T. S., Xue, Y., Carranza, A., and Garcia-Garibay, M. A. (2017) Stereospecific photochemistry of Δ^2-1,2,3-triazolines in solution and in the solid state: scope and mechanistic studies. *Photochem. Photobiol. Sci. 16*, 1458-1463.
(46) Chen, Y. J., Hung, H. C., Sha, C. K., and Chung, W. S. (2010) Photochemistry of benzene and quinoxaline fused Δ^2–1,2,3–triazolines and their trapping products. *Tetrahedron 66*, 176-182.
(47) Bailey, A. S. and Wedgwood, J. J. (1968) The reaction of picryl azide with olefins. *J. Chem. Soc. (C)*, 682-684.
(48) Shao, Y., Molnar, L. F., Jung, Y., Kussmann, J., Ochsenfeld, C., Brown, S. T., Gilbert, A. T. B., Slipchenko, L. V., Levchenko, S. V., O'Neill, D. P., et al. (2006) Advances in methods and algorithms in a modern quantum chemistry program package. *Phys. Chem. Chem. Phys. 8*, 3172-3191.
(49) Halgren, T. A. (1996) Merck molecular force field. I. Basis, form, scope, parameterization, and performance of MMFF94. *J. Comput. Chem. 17*, 490-519.
(50) Frisch, M. J. T., G. W.; Schlegel, H. B.; Scuseria, G. E.; Robb, M. A.; Cheeseman, J. R.; Scalmani, G.; Barone, V.;

Mennucci, B.; Petersson, G. A., et al. (2009), Gaussian 09, revision D.01, Gaussian, Inc., Wallingford CT.

TOC Graphic:

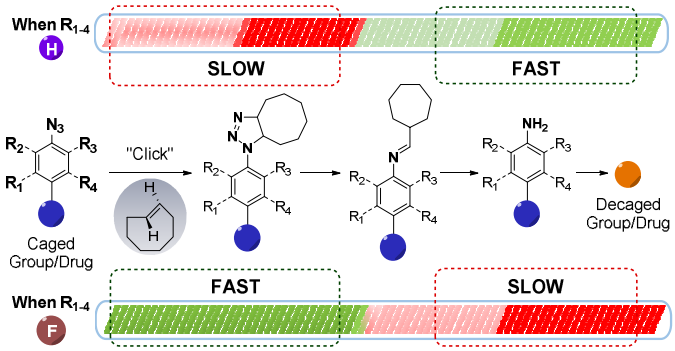
When R1-4
H
SLOW
FAST
N3
R2
R3
R1
R4
Caged
Group/Drug
"Click"
H
H
N
N
N
NH2
Decaged
Group/Drug
FAST
SLOW
When R1-4
F